Single-loop multiple-pulse nonadiabatic holonomic quantum gates

Emmi Herterich and Erik Sjöqvist*

Department of Physics and Astronomy, Uppsala University, Box 516, Se-751 20 Uppsala, Sweden

(Received 26 August 2016; published 9 November 2016)

Nonadiabatic holonomic quantum computation provides the means to perform fast and robust quantum gates by utilizing the resilience of non-Abelian geometric phases to fluctuations of the path in state space. While the original scheme [E. Sjöqvist *et al.*, New J. Phys. **14**, 103035 (2012)] needs two loops in the Grassmann manifold (i.e., the space of computational subspaces of the full state space) to generate an arbitrary holonomic one-qubit gate, we propose single-loop one-qubit gates that constitute an efficient universal set of holonomic gates when combined with an entangling holonomic two-qubit gate. Our one-qubit gate is realized by dividing the loop into path segments, each of which is generated by a Λ-type Hamiltonian. We demonstrate that two path segments are sufficient to realize arbitrary single-loop holonomic one-qubit gates. We describe how our scheme can be implemented experimentally in a generic atomic system exhibiting a three-level Λ-coupling structure by utilizing carefully chosen laser pulses.

DOI: 10.1103/PhysRevA.94.052310

I. INTRODUCTION

Holonomic quantum computation (HQC) is the idea that quantum information processing can be performed by means of non-Abelian geometric phases. It was first proposed [1] for adiabatic holonomies [2] and subsequently generalized [3] to nonadiabatic non-Abelian geometric phases [4]. An important feature of HQC is the inherent robustness of geometric phases under fluctuations of the path in state space [5,6].

A key ingredient of HQC is the removal of dynamical phase effects during the execution of quantum gates. In the nonadiabatic case, which is the focus of the present paper, this is achieved in a three-level Λ system, where the two levels encoding a qubit are coupled to an excited state by external field pulses. Nonadiabatic HQC in this configuration has been realized experimentally for a superconducting artificial atom [7], NMR [8], and nitrogen-vacancy (NV) centers in diamond [9,10]. The Λ-system-based HQC has been combined with decoherence-free subspaces [11–16], noiseless subsystems [17], and dynamical decoupling [18]. The nonadiabatic property makes it possible to shorten the exposure to undesired external influences [3,19].

The essential geometric structure of nonadiabatic HQC is the complex Grassmann manifold $\mathcal{G}(N;K)$, i.e., the space of K-dimensional subspaces of an N-dimensional state space [20]. A loop in the Grassmannian generates a holonomic quantum gate acting on the target computational subspace encoded at the common start and end point.

The Λ-system-based holonomic gates in Ref. [3] utilize resonant laser pulses. Here, two distinct loops in the corresponding Grassmannian $\mathcal{G}(3;2)$ are needed to perform an arbitrary holonomic one-qubit gate. Experimentally, the two loops correspond to two consecutive laser pulse pairs of arbitrary shape.

The need for two loops in order to implement an arbitrary holonomic one-qubit gate is an apparent drawback as it doubles the exposure time to various error sources. This motivates attempts to try to reduce the number of loops. It has recently been shown [21,22] that an arbitrary one-qubit gate can be achieved for a single loop by using off-resonant laser pulses. However, this off-resonant scheme has two disadvantages. First, it requires square pulses, a restriction that blocks the possibility to optimize robustness by tailoring the pulse shape; second, the small-rotation-angle limit would correspond to either very short pulses or small field amplitudes, both of which would lead to unstable gate operations.

Here, we demonstrate that these problems can be resolved. To this end, we propose a single-loop multiple-pulse scheme, in which the loop is divided into segments. Our scheme is conceptually akin to the "orange-slice" path on the Bloch sphere commonly used when observing the Abelian geometric phase in quantum optics experiments [23–26]. We demonstrate that our proposed scheme is able to perform arbitrary holonomic one-qubit gates for fewer loops in the Grassmannian than in the original scheme [3], while keeping the full flexibility concerning the choice of laser pulse shape and pulse duration. Universal HQC can be achieved by combining our holonomic one-qubit gate with an entangling holonomic two-qubit gate (e.g., [3,27]).

The outline of the paper is as follows. The next section reviews earlier versions of Λ-system-based holonomic gates. Section III outlines our single-loop multiple-pulse scheme, first by describing the general idea and thereafter by demonstrating that an arbitrary holonomic one-qubit gate can be realized by dividing the loop into just two path segments. In Sec. IV, we delineate how our scheme can be implemented experimentally. The paper ends with the conclusions.

II. HOLONOMIC GATES IN THE Λ SYSTEM

In the Λ configuration, a laser pulse pair induces transitions between the qubit states $|0\rangle$ and $|1\rangle$ and the excited state $|e\rangle$ of a generic three-level system. This is described by the Hamiltonian (we set $\hbar = 1$ from now on)

$$\mathcal{H}(t) = \Delta_0 |0\rangle \langle 0| + \Delta_1 |1\rangle \langle 1| + \Upsilon_0(t) |e\rangle \langle 0| + \Upsilon_1(t) |e\rangle \langle 1| + \text{H.c.}, \quad (1)$$

where we have used the rotating-wave approximation in the interaction picture. The complex-valued ratio $\Upsilon_0(t)/\Upsilon_1(t)$

*erik.sjoqvist@physics.uu.se

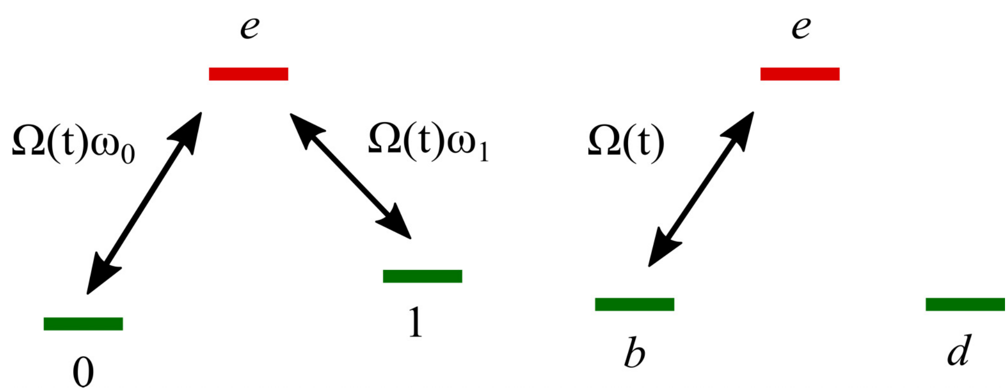

FIG. 1. The Λ system. In the left panel, we see how the qubit states $|0\rangle$ and $|1\rangle$, defining our target computational subspace, are controlled by the laser parameters $\Omega(t)\omega_0$ and $\Omega(t)\omega_1$, respectively. The dynamics can be understood as Rabi oscillations between the bright state $|b\rangle = \omega_0^* |0\rangle + \omega_1^* |1\rangle$ and excited state $|e\rangle$, while the dark state $|d\rangle = -\omega_1 |0\rangle + \omega_0 |1\rangle$ decouples from the system, as shown in the right panel.

describes the relative amplitude and phase between the laser pulses; Δ_p, with $p = 0,1$, are detunings.

Holonomic quantum information processing in the Λ system is implemented by applying the laser pulses simultaneously and on resonance [3]. In other words, $\Upsilon_p(t) = \Omega(t)\omega_p$ and $\Delta_p = 0$. Here, $\Omega(t)$ is real valued and has nonvanishing support over the duration τ of the pulse pair. The time-independent ω_p are assumed to satisfy the normalization relation $|\omega_0|^2 + |\omega_1|^2 = 1$.

To see how these parameter choices implement a purely holonomic gate acting on Span$\{|0\rangle, |1\rangle\}$, it is convenient first to express the Hamiltonian in terms of the dark and bright states $|d\rangle = -\omega_1 |0\rangle + \omega_0 |1\rangle$ and $|b\rangle = \omega_0^* |0\rangle + \omega_1^* |1\rangle$, respectively. One thereby finds

$$\mathcal{H}(t) = \Omega(t)(|e\rangle\langle b| + |b\rangle\langle e|) \equiv \Omega(t)H, \tag{2}$$

which shows that the evolution can be understood as Rabi oscillations between $|b\rangle$ and $|e\rangle$ with frequency $\Omega(t)$, while $|d\rangle$ decouples from the system. The Λ configuration in the $|0\rangle, |1\rangle$ and $|d\rangle, |b\rangle$ representations is shown in Fig. 1. The Hamiltonian in Eq. (2) moves the qubit subspace Span$\{|0\rangle, |1\rangle\}$ in the full state space Span$\{|0\rangle, |1\rangle, |e\rangle\}$, a process that can be viewed as a path in the Grassmannian $\mathcal{G}(3;2)$. Each point along the path in $\mathcal{G}(3;2)$ is spanned by the vectors

$$\begin{aligned} |\psi_d(a)\rangle &= \mathcal{U}(a,0)|d\rangle = |d\rangle, \\ |\psi_b(a)\rangle &= \mathcal{U}(a,0)|b\rangle = \cos(a)|b\rangle - i\sin(a)|e\rangle, \end{aligned} \tag{3}$$

where

$$a = \int_0^t \Omega(t')dt' \tag{4}$$

is the pulse area and $\mathcal{U}(a,0) = \exp(-iaH)$ is the time-evolution operator. A full loop $C_{\mathbf{n}}$ in the Grassmannian is realized when $a \equiv a_1 = \pi$. The transformation on the one-qubit subspace is purely holonomic (i.e., depends only on $C_{\mathbf{n}}$) as the dynamical matrix elements $\langle\psi_k(a)|\mathcal{H}(t)|\psi_l(a)\rangle$, with $k,l = b,d$, all vanish for $a \in [0,\pi]$. Explicitly, one finds [3,28]

$$U(C_{\mathbf{n}}) = \mathcal{U}(\pi,0)\mathbb{P}(0) = ie^{-i\frac{1}{2}\pi\mathbf{n}\cdot\boldsymbol{\sigma}} = \mathbf{n}\cdot\boldsymbol{\sigma}, \tag{5}$$

where $\mathbf{n} = (\sin\theta\cos\phi, \sin\theta\sin\phi, \cos\theta)$ is a unit vector defined by $\omega_0/\omega_1 = -e^{i\phi}\tan\frac{\theta}{2}$, $\mathbb{P}(0) = |d\rangle\langle d| + |b\rangle\langle b| = |0\rangle\langle 0| + |1\rangle\langle 1|$ is the projection operator on the target computational subspace encoding the qubit, and $\boldsymbol{\sigma} = (\sigma_x,\sigma_y,\sigma_z)$ are the standard Pauli operators expressed in the $|0\rangle, |1\rangle$ basis. The resulting unitary transformation $U(C_{\mathbf{n}})$ is the holonomic one-qubit gate associated with the loop $C_{\mathbf{n}}$.

The holonomy in Eq. (5) shows that a single pulse pair can generate only traceless one-qubit gates. To achieve arbitrary holonomic gates, it is necessary to apply two consecutive laser pulse pairs, each with pulse area π, which corresponds to traversing two loops in the Grassmannian. To see this, assume that the two pulse pairs generate loops $C_{\mathbf{n}_1}$ and $C_{\mathbf{n}_2}$, characterized by laser parameters that correspond to unit vectors $\mathbf{n}_1$ and $\mathbf{n}_2$; the resulting composite holonomy transformation becomes

$$\begin{aligned} U(C) &= U(C_{\mathbf{n}_2})U(C_{\mathbf{n}_1}) \\ &= \mathbf{n}_1\cdot\mathbf{n}_2\,\mathbb{P}(0) - i(\mathbf{n}_1\times\mathbf{n}_2)\cdot\boldsymbol{\sigma}. \end{aligned} \tag{6}$$

This is an arbitrary SU(2) transformation that rotates the qubit by an angle $2\arccos(\mathbf{n}_1\cdot\mathbf{n}_2)$ around the normal of the plane spanned by $\mathbf{n}_1$ and $\mathbf{n}_2$.

The need for two loops is an apparent drawback as it doubles the exposure time to various error sources. Thus, it is desirable to find methods that can realize holonomic one-qubit gates for a single loop in the Grassmannian. It was recently shown [21,22] that off-resonant, equally detuned laser pulses can be used to implement arbitrary single-loop holonomic one-qubit gates. This is described by the Hamiltonian

$$\mathcal{H}_\Delta(t) = \Delta|e\rangle\langle e| + \Omega(t)(|e\rangle\langle b| + |b\rangle\langle e|), \tag{7}$$

with a trivial shift of the zero-point energy and Δ being the detuning [29]. In order to preserve the geometric character of the evolution, the Hamiltonian needs to commute with itself during the pulse, which implies that $\Omega(t)$ must be square shaped; that is, $\Omega(t) = \Omega_0$ for $0 \leqslant t \leqslant \tau$ and zero otherwise. The evolution becomes cyclic, corresponding to a loop $C_{\mathbf{n};\Delta}$ in the Grassmannian if

$$\tau = \frac{2\pi}{\sqrt{\Delta^2 + 4\Omega_0^2}}. \tag{8}$$

One finds

$$U(C_{\mathbf{n};\Delta}) = e^{i\frac{1}{2}(\pi-\chi)}e^{-i\frac{1}{2}(\pi-\chi)\mathbf{n}\cdot\boldsymbol{\sigma}}, \tag{9}$$

where

$$\chi = \frac{\pi\Delta}{\sqrt{\Delta^2 + 4\Omega_0^2}}. \tag{10}$$

The gate $U(C_{\mathbf{n};\Delta})$ is an arbitrary holonomic one-qubit gate as the rotation angle $\pi - \chi$ can be varied between zero and π by decreasing $\Delta/(2\Omega_0)$ from infinity to zero. As a consistency check, we may note that $U(C_{\mathbf{n};\Delta})$ reduces to $U(C_{\mathbf{n}})$ in the $\Delta/(2\Omega_0) \to 0$ limit.

Although $U(C_{\mathbf{n};\Delta})$ covers all one-qubit gates, it suffers from two disadvantages. First, if $\Delta \neq 0$, then the pulse must be square shaped in order to preserve the geometric character of the gate, which is a practical limitation as full shape flexibility is an important feature needed to optimize robustness to different kinds of errors (see, e.g., [30]). Second, the small-rotation-angle limit is achieved for large $\Delta/(2\Omega_0)$. This can be reached either by using a large Δ and thereby a small τ, which makes the gate highly unstable to small perturbations in the run time [31], or by using a small Ω_0, which introduces an instability similar to fluctuations in the field amplitude. In the following section, we demonstrate a multiple-pulse method to realize arbitrary single-loop holonomic one-qubit gates, which avoids these disadvantages.

III. SINGLE-LOOP MULTIPLE-PULSE SCHEME

A. General setting

Consider a path in $\mathcal{G}(3;2)$ divided into L segments $C_1,\ldots,C_L$, generated by L pulse pairs with pulse areas $a_1,\ldots,a_L$. Figure 2 schematically depicts such a division when $C_1 * \cdots * C_L$ is a loop and $L = 3$. The process of dividing the path can be described as the following iterative procedure:

(i) The first path segment starts at the target computational subspace $\text{Span}\{|b\rangle, |d\rangle\} = \text{Span}\{|0\rangle, |1\rangle\}$ and is generated by the zero-detuned (resonant) Hamiltonian $\mathcal{H}_1(t)$, which is identical to $\mathcal{H}(t)$ in Eq. (2).

(ii) The initial point $\text{Span}\{|\psi_{n;b}(0)\rangle, |\psi_{n;d}(0)\rangle\}$ of the nth path segment coincides with the final point $\text{Span}\{|\psi_{n-1;b}(a_{n-1})\rangle, |\psi_{n-1;d}(a_{n-1})\rangle\}$ of the $(n-1)$th path segment for $n = 2,\ldots,L$.

(iii) The resonant Hamiltonian driving the evolution along the nth path segment reads

$$\mathcal{H}_n(t) = \Omega_n(t)[|\psi_{n;e}(0)\rangle\langle\psi_{n;b}(0)| + |\psi_{n;b}(0)\rangle\langle\psi_{n;e}(0)|] \equiv \Omega_n(t)H_n, \tag{11}$$

where

$$|\psi_{n;k}(0)\rangle = V_n|\psi_{n-1;k}(a_{n-1})\rangle, \quad k = b,d, \tag{12}$$

and $a_{n-1} = \int_0^{\tau_{n-1}} \Omega_{n-1}(t)dt$, with τ_{n-1} being the corresponding run time. Here, the basis transformation V_n acts unitarily on the final subspace of the $(n-1)$th segment, which further implies that $V_n|\psi_{n-1;e}(a_{n-1})\rangle = |\psi_{n-1;e}(a_{n-1})\rangle$. Physically, V_n defines the discrete changes of the external laser fields when moving from C_{n-1} to C_n.

The time-evolution operator along the nth path segment evaluated at pulse area a_n takes the form [19]

$$\mathcal{U}_n(a_n,0) = e^{-ia_nH_n} = |\psi_{n;d}(0)\rangle\langle\psi_{n;d}(0)| + \cos a_n[\hat{1} - |\psi_{n;d}(0)\rangle\langle\psi_{n;d}(0)|]$$

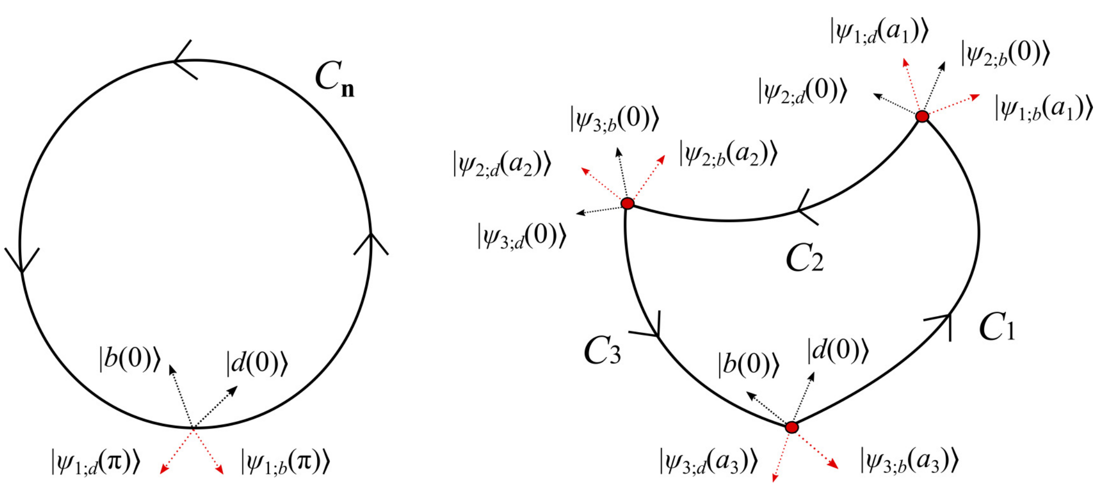

FIG. 2. The single-loop multiple-pulse scheme in the Λ system. The left panel shows the case of a loop generated by a single pulse pair. The initial point in the Grassmannian $\mathcal{G}(3;2)$ spanned by the vectors $|k\rangle$, $k = b,d$, where $|b\rangle = \omega_0^*|0\rangle + \omega_1^*|1\rangle$ and $|d\rangle = -\omega_1|0\rangle + \omega_0|1\rangle$, makes one full revolution by following the path generated by the Λ Hamiltonian $\mathcal{H}(t) = \Omega(t)(|e\rangle\langle b| + |b\rangle\langle e|)$. This induces the holonomic one-qubit transformation $|k\rangle \mapsto |\psi_k\rangle = U(C_{\mathbf{n}})|k\rangle$, with $\mathbf{n}$ being determined by the laser parameters ω_0 and ω_1. The closing of the path is ensured by choosing pulse area $a \equiv a_1 = \int_0^\tau \Omega(t)dt = \pi$. The right panel visualizes the multiple-pulse scheme, in which the loop is divided into path segments. Here, the initial subspace moves along the first path segment C_1 under $\mathcal{H}_1(t) = \mathcal{H}(t)$ to a point spanned by $|\psi_{1;k}(a_1)\rangle$ by choosing pulse area $a_1 \neq \pi$. A unitary transformation, $|\psi_{1;k}(a_1)\rangle \mapsto |\psi_{2;k}(0)\rangle$ and $|\psi_{1;e}(a_1)\rangle \mapsto |\psi_{2;e}(0)\rangle = |\psi_{1;e}(a_1)\rangle$, defines a new Λ Hamiltonian $\mathcal{H}_2(t) = \Omega_2(t)[|\psi_{2;e}(0)\rangle\langle\psi_{2;b}(0)| + |\psi_{2;b}(0)\rangle\langle\psi_{2;e}(0)|]$ that generates the second path segment C_2. This procedure is repeated L times (here, the $L = 3$ case is shown). If the final point of the Lth segment coincides with $\text{Span}\{|b\rangle, |d\rangle\} = \text{Span}\{|0\rangle, |1\rangle\}$, then $C_1 * \cdots * C_L$ forms a loop. In this case, the resulting transformation $|k\rangle \mapsto |\psi_{L;k}(a_L)\rangle = U(C_1 * \cdots * C_L)|k\rangle$ is unitary and constitutes our holonomic single-loop multiple-pulse one-qubit gate.

$$- i \sin a_n [|\psi_{n;e}(0)\rangle \langle\psi_{n;b}(0)| + |\psi_{n;b}(0)\rangle \langle\psi_{n;e}(0)|]. \quad (13)$$

Due to the Λ structure of H_n, it follows that the evolution of the computational subspace is purely geometric along all path segments. We thus find the holonomy [28]

$$U(C_1 * \cdots * C_L) = \mathcal{U}_L(a_L,0)\cdots\mathcal{U}_1(a_1,0)\mathbb{P}(0). \quad (14)$$

By carefully choosing laser parameters so that $C_1 * \cdots * C_L$ forms a loop, $U(C_1 * \cdots * C_L)$ is a unitary operator acting on Span$\{|0\rangle, |1\rangle\}$. In such a case, $U(C_1 * \cdots * C_L)$ is our one-qubit gate.

B. $L = 2$ holonomic gates

We now demonstrate that two pulse pairs ($L = 2$) with $a_1 = a_2 = \pi/2$ are sufficient to construct an arbitrary holonomic one-qubit quantum gate by traversing a single loop in $\mathcal{G}(3;2)$.

Our starting point is $|\psi_{1;e}(0)\rangle = |e\rangle$, $|\psi_{1;b}(0)\rangle = |b\rangle$, and $|\psi_{1;d}(0)\rangle = |d\rangle$, where the two latter vectors span the target computational subspace. By directly evaluating the time-evolution operator in Eq. (13) at $a_1 = \pi/2$, we obtain

$$\mathcal{U}_1(\pi/2,0) = |d\rangle\langle d| - i(|e\rangle\langle b| + |b\rangle\langle e|), \quad (15)$$

which yields

$$|\psi_{1;e}(\pi/2)\rangle = \mathcal{U}_1(\pi/2,0)|e\rangle = -i|b\rangle,$$
$$|\psi_{1;b}(\pi/2)\rangle = \mathcal{U}_1(\pi/2,0)|b\rangle = -i|e\rangle,$$
$$|\psi_{1;d}(\pi/2)\rangle = \mathcal{U}_1(\pi/2,0)|d\rangle = |d\rangle. \quad (16)$$

The next step is to find the vectors $|\psi_{2,k}(0)\rangle$ spanning the initial point of the second path segment C_2. We can make a nontrivial choice of these vectors so that the final point of C_2 coincides with the initial point of C_1, i.e., so that $C_1 * C_2$ forms a loop. The choice is

$$|\psi_{2;e}(0)\rangle = V_2|\psi_{1;e}(\pi/2)\rangle = -i|b\rangle,$$
$$|\psi_{2;b}(0)\rangle = V_2|\psi_{1;b}(\pi/2)\rangle = -ie^{i\eta}|e\rangle, \quad (17)$$
$$|\psi_{2;d}(0)\rangle = V_2|\psi_{1;d}(\pi/2)\rangle = e^{-i\eta}|d\rangle,$$

as given by the basis transformation

$$V_2 = |\psi_{1;e}(\pi/2)\rangle\langle\psi_{1;e}(\pi/2)| + e^{i\eta}|\psi_{1;b}(\pi/2)\rangle\langle\psi_{1;b}(\pi/2)| + e^{-i\eta}|\psi_{1;d}(\pi/2)\rangle\langle\psi_{1;d}(\pi/2)|$$
$$= |b\rangle\langle b| + e^{i\eta}|e\rangle\langle e| + e^{-i\eta}|d\rangle\langle d|. \quad (18)$$

The resulting Hamiltonian for the second pulse thus reads

$$\mathcal{H}_2(t) = \Omega_2(t)(e^{-i\eta}|b\rangle\langle e| + e^{i\eta}|e\rangle\langle b|)$$
$$\equiv \Omega_2(t)H_2, \quad (19)$$

which generates the time-evolution operator

$$\mathcal{U}_2(\pi/2,0) = |d\rangle\langle d| - i(e^{-i\eta}|b\rangle\langle e| + e^{i\eta}|e\rangle\langle b|) \quad (20)$$

when evaluated at $a_2 = \pi/2$. By taking into account the explicit form of the bright state, we see that $\mathcal{H}_2(t)$ is equivalent to a shift of the two laser parameters ω_p by the same phase η, i.e., $\omega_p \mapsto e^{i\eta}\omega_p$.

Consecutive application of $\mathcal{U}_1(\pi/2,0)$ and $\mathcal{U}_2(\pi/2,0)$ generates a loop $C_1 * C_2$ in the Grassmannian. Thus,

$$U(C_1 * C_2) = \mathcal{U}_2(\pi/2,0)\mathcal{U}_1(\pi/2,0)\mathbb{P}(0) \quad (21)$$

is unitary and constitutes the holonomic one-qubit quantum gate. By inserting Eqs. (15) and (20) into Eq. (21), we obtain

$$U(C_1 * C_2) = |d\rangle\langle d| - e^{-i\eta}|b\rangle\langle b|$$
$$= e^{i\frac{1}{2}(\pi-\eta)}e^{-i\frac{1}{2}(\pi-\eta)\mathbf{n}\cdot\boldsymbol{\sigma}}. \quad (22)$$

The factor $e^{i\frac{1}{2}(\pi-\eta)}$ is a global phase factor that can be ignored. The operator $e^{-i\frac{1}{2}(\pi-\eta)\mathbf{n}\cdot\boldsymbol{\sigma}}$ corresponds to a rotation around $\mathbf{n}$ by an angle $\pi - \eta$, which should be compared to the rotation around $\mathbf{n}_1 \times \mathbf{n}_2/|\mathbf{n}_1 \times \mathbf{n}_2|$ by the angle $2\arccos(\mathbf{n}_1 \cdot \mathbf{n}_2)$ obtained by traversing two loops in the original π pulse scheme, as given by Eq. (6).

The holonomic gate $U(C_1 * C_2)$ reaches all possible one-qubit transformations by separately varying the phase shift η and the laser parameters $\mathbf{n}$. In contrast to the off-resonant scheme proposed in Refs. [21,22], our gate preserves its geometric character for any pulse shape. It is essential in the proposed $L = 2$ scheme that the two pulse pairs both have area $\pi/2$ in order for the two path segments to form a loop in the Grassmannian [32]. We further note that the rotation angle $\pi - \eta$ is independent of the duration of the pulses, which implies that the small-angle limit is achievable without violating the rotating-wave approximation. Thus, we conclude that our holonomic one-qubit gate resolves the problems of the off-resonant scheme [21,22], still maintaining the single-loop advantage over the original proposal of Ref. [3].

IV. EXPERIMENTAL IMPLEMENTATION

The $L = 2$ holonomic gates can be implemented experimentally in electric dipole transitions generated by four appropriately phase shifted laser pulses in a generic atomic three-level systems. The four laser pulses should be applied as two consecutive pairs, as shown in Fig. 3. The first pair is given by the oscillating electric fields $\mathbf{E}_{1;p}(t) = \boldsymbol{\epsilon}_p g_1(t)\cos(f_p t + \varphi_p)$, with $p = 0,1$ and $g_1(t)$ being the envelope function describing the common shape and duration of the pulses. Similarly, the second pulse pair is given by $\mathbf{E}_{2;p}(t) = \boldsymbol{\epsilon}_p g_2(t)\cos(f_p t + \varphi_p + \eta)$ and should not overlap with the first pulse pair [thus, $g_1(t)$ and $g_2(t)$ should be mutually nonoverlapping but have the same shape]. The polarization $\boldsymbol{\epsilon}_p$ is chosen so as to allow for only the $|p\rangle \leftrightarrow |e\rangle$ transition by utilizing appropriate selection rules. The ratio $|\boldsymbol{\epsilon}_0|^2/|\boldsymbol{\epsilon}_1|^2$ describes the relative intensity of the two laser pulses. We assume that the oscillation frequencies f_p are tuned on resonance with the transition frequencies ν_{ep}, given by the bare Hamiltonian $\mathcal{H}_{\text{bare}} = -\nu_{e0}|0\rangle\langle 0| - \nu_{e1}|1\rangle\langle 1|$, for which the energy of the excited state is taken as the zero point.

Now, in the interaction picture, we find

$$\tilde{H}_1(t) = \Omega_1(t)[\omega_0(1 + e^{-2i\nu_{e0}t})|e\rangle\langle 0| + \omega_1(1 + e^{-2i\nu_{e1}t})|e\rangle\langle 1| + \text{H.c.}],$$
$$\tilde{H}_2(t) = \Omega_2(t)[\omega_0(e^{i\eta} + e^{-2i\nu_{e0}t - i\eta})|e\rangle\langle 0| + \omega_1(e^{i\eta} + e^{-2i\nu_{e1}t - i\eta})|e\rangle\langle 1| + \text{H.c.}]. \quad (23)$$

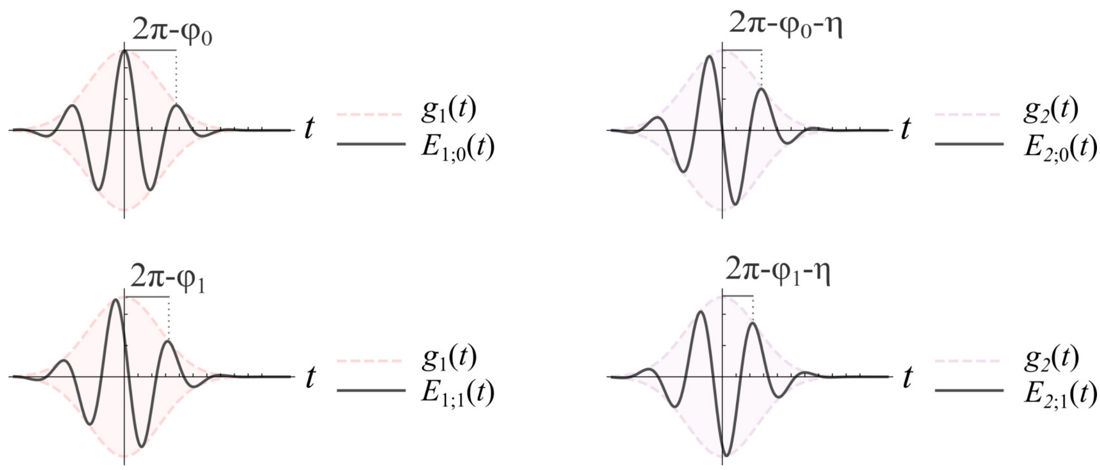

FIG. 3. Laser pulses that implement $L = 2$ holonomic gates. The first (second) pulse pair is shown in the left (right) panel. The pulses within each pair are applied simultaneously, while the pairs are mutually nonoverlapping in time but have the same shape. The oscillating solid lines are the pulses $E_{1;p}(t) = g_1(t)\cos(f_p t + \varphi_p) \propto |\mathbf{E}_{1;p}(t)|$ and $E_{2;p}(t) = g_2(t)\cos(f_p t + \varphi_p + \eta) \propto |\mathbf{E}_{2;p}(t)|$, $p = 0,1$, restricted by the dashed curves $\pm g_1(t)$ and $\pm g_2(t)$, respectively. These pulses realize an $L = 2$ holonomic one-qubit gate provided the area of the envelope functions $g_n(t)$, $n = 1,2$, is chosen so as to implement $\frac{\pi}{2}$ pulses.

Here, $\Omega_n(t)\omega_p = e^{i\varphi_p} \langle e| \boldsymbol{\mu} \cdot \boldsymbol{\epsilon}_p |p\rangle g_n(t)/2$, with $n = 1,2$ and $\boldsymbol{\mu}$ being the electric dipole operator, which determine the polar angles θ and ϕ of $\mathbf{n}$ according to

$$e^{i(\varphi_0-\varphi_1)} \frac{\langle e| \boldsymbol{\mu} \cdot \boldsymbol{\epsilon}_0 |0\rangle}{\langle e| \boldsymbol{\mu} \cdot \boldsymbol{\epsilon}_1 |1\rangle} = -e^{i\phi} \tan\frac{\theta}{2}. \quad (24)$$

By neglecting the rapidly oscillating terms $e^{\pm 2i\nu_{ep}t}$ and $e^{\pm i(2\nu_{ep}t+\eta)}$ (rotating-wave approximation), we see that $\tilde{H}_n(t)$ coincides with $\mathcal{H}_n(t)$, thus demonstrating that the holonomic one-qubit gate in Eq. (22) can be realized in this physical setting.

The superconducting artificial atom experiment in Ref. [7] used pulse durations τ on the order of 40 ns and transition frequencies $\nu_{ep}/(2\pi)$ on the order of 8 GHz, which is well within the rotating-wave-approximation regime $[2\pi/(\nu_{ep}\tau) \approx 0.003 \ll 1]$. A multiple-pulse variant of this experiment can therefore implement stable holonomic gates. For instance, a phase-shift gate $|x\rangle \mapsto e^{ix\zeta} |x\rangle$, where $x = 0,1$, in this setup could be implemented by applying two $\pi/2$ laser pulse pairs with $\omega_0 = 1$, where the second pulse pair is phase shifted by $\eta = \pi - \zeta$ relative to the first pulse pair.

We note that the phase shift η has only physical significance as a relative phase shift between the two pulse pairs. In other words, if the same phase shift had been applied in the original single-loop scheme of Ref. [3], no physical effect would have been seen. In fact, the only parameters that matter for the evolution in the original scheme are the pulse area and the ratio ω_0/ω_1, where the latter is clearly unchanged under the phase shift $\omega_p \mapsto \omega_p e^{i\eta}$.

V. CONCLUSIONS

Nonadiabatic holonomic quantum computation can be implemented by tailoring amplitude, phase, and area of laser pulses driving a Λ system. Here, we have proposed a single-loop multiple-pulse scheme that implements holonomic gates in this system. Specifically, we have demonstrated that the simplest nontrivial case corresponding to two pulse pairs ($L = 2$) is sufficient to realize an arbitrary single-loop one-qubit gate. By combining our one-qubit gate with an entangling holonomic two-qubit gate, an efficient universal set of holonomic gates can be realized.

Our scheme avoids the drawbacks of earlier versions of nonadiabatic holonomic quantum computation. It minimizes the exposure time to errors but keeps the full flexibility concerning the choice of laser pulse shape and pulse duration. We have further outlined an experimental setting involving a combination of carefully chosen laser pulses.

We note that the $L = 2$ gates involve control of two new parameters: the phase shift η and an additional pulse area. Thus, an optimal strategy uses the multiple-pulse one-loop scheme only to implement one-qubit gates with nonvanishing trace (such as phase shifts); for gates with vanishing trace (such as bit flip and Hadamard) the original π scheme of Ref. [3] is preferable.

The $L = 2$ case can be extended to any number of pulse pairs. The resulting paths would explore larger regions of the underlying Grassmann manifold $\mathcal{G}(3;2)$ and may therefore provide further insight into the geometrical structure of the $\mathcal{G}(3;2)$ holonomy. Thus, from a fundamental point of view, experimental and theoretical study of the $L \geqslant 3$ case is of interest.

ACKNOWLEDGMENT

E.S. acknowledges support from the Swedish Research Council through Grant No. D0413201.

[1] P. Zanardi and M. Rasetti, Holonomic quantum computation, Phys. Lett. A **264**, 94 (1999).
[2] F. Wilczek and A. Zee, Appearance of Gauge Structure in Simple Dynamical Systems, Phys. Rev. Lett. **52**, 2111 (1984).
[3] E. Sjöqvist, D. M. Tong, L. M. Andersson, B. Hessmo, M. Johansson, and K. Singh, Non-adiabatic holonomic quantum computation, New J. Phys. **14**, 103035 (2012).
[4] J. Anandan, Non-adiabatic non-Abelian geometric phase, Phys. Lett. A **133**, 171 (1988).
[5] J. Pachos and P. Zanardi, Quantum holonomies for quantum computing, Int. J. Mod. Phys. B **15**, 1257 (2001).
[6] P. Solinas, M. Sassetti, P. Truini, and N. Zanghì, On the stability of quantum holonomic gates, New J. Phys. **14**, 093006 (2012).
[7] A. A. Abdumalikov, Jr., J. M. Fink, K. Juliusson, M. Pecha, S. Berger, A. Wallraff, and S. Filipp, Experimental realization of non-Abelian non-adiabatic geometric gates, Nature (London) **496**, 482 (2013).
[8] G. R. Feng, G. F. Xu, and G. L. Long, Experimental Realization of Nonadiabatic Holonomic Quantum Computation, Phys. Rev. Lett. **110**, 190501 (2013).
[9] S. Arroyo-Camejo, A. Lazariev, S. W. Hell, and G. Balasubramanian, Room temperature high-fidelity holonomic single-qubit gate on a solid-state spin, Nat. Commun. **5**, 4870 (2014).
[10] C. Zu, W.-B. Wang, L. He, W.-G. Zhang, C.-Y. Dai, F. Wang, and L.-M. Duan, Experimental realization of universal geometric quantum gates with solid-state spins, Nature (London) **514**, 72 (2014).
[11] G. F. Xu, J. Zhang, D. M. Tong, E. Sjöqvist, and L. C. Kwek, Nonadiabatic Holonomic Quantum Computation in Decoherence-Free Subspaces, Phys. Rev. Lett. **109**, 170501 (2012).
[12] G. F. Xu and G. L. Long, Universal Nonadiabatic Geometric Gates in Two-Qubit Decoherence-Free Subspaces, Sci. Rep. **4**, 6814 (2014).
[13] Z.-T. Liang, Y.-X. Du, W. Huang, Z.-Y. Xue, and H. Yan, Nonadiabatic holonomic quantum computation in decoherence-free subspaces with trapped ions, Phys. Rev. A **89**, 062312 (2014).
[14] Z.-Y. Xue, J. Zhou, and Z. D. Wang, Universal holonomic quantum gates in decoherence-free subspace on superconducting circuits, Phys. Rev. A **92**, 022320 (2015).
[15] J. Zhou, W.-C. Yu, Y.-M. Gao, and Z.-Y. Xue, Cavity QED implementation of non-adiabatic holonomies for universal quantum gates in decoherence-free subspaces with nitrogen-vacancy centers, Opt. Express **23**, 14027 (2015).
[16] Z.-Y. Xue, J. Zhou, Y.-M. Chu, and Y. Hu, Nonadiabatic holonomic quantum computation with all-resonant control, Phys. Rev. A **94**, 022331 (2016).
[17] J. Zhang, L. C. Kwek, E. Sjöqvist, D. M. Tong, and P. Zanardi, Quantum computation in noiseless subsystems with fast non-Abelian holonomies, Phys. Rev. A **89**, 042302 (2014).
[18] G. F. Xu and G. L. Long, Protecting geometric gates by dynamical decoupling, Phys. Rev. A **90**, 022323 (2014).
[19] M. Johansson, E. Sjöqvist, L. M. Andersson, M. Ericsson, B. Hessmo, K. Singh, and D. M. Tong, Robustness of nonadiabatic holonomic gates, Phys. Rev. A **86**, 062322 (2012).
[20] I. Bengtsson and K. Życzkowski, *Geometry of Quantum States* (Cambridge University Press, Cambridge, 2006), Chap. 4.9.
[21] G. F. Xu, C. L. Liu, P. Z. Zhao, and D. M. Tong, Nonadiabatic holonomic gates realized by a single-shot implementation, Phys. Rev. A **92**, 052302 (2015).
[22] E. Sjöqvist, Nonadiabatic holonomic single-qubit gates in off-resonant Λ systems, Phys. Lett. A **380**, 65 (2016).
[23] P. G. Kwiat and R. Y. Chiao, Observation of a Nonclassical Berry's Phase for the Photon, Phys. Rev. Lett. **66**, 588 (1991).
[24] B. E. Allman, H. Kaiser, S. A. Werner, A. G. Wagh, V. C. Rakhecha, and J. Summhammer, Observation of geometric and dynamical phases by neutron interferometry, Phys. Rev. A **56**, 4420 (1997).
[25] J. Du, P. Zou, M. Shi, L. C. Kwek, J.-W. Pan, C. H. Oh, A. Ekert, D. K. L. Oi, and M. Ericsson, Observation of Geometric Phases for Mixed States Using NMR Interferometry, Phys. Rev. Lett. **91**, 100403 (2003).
[26] L. Rippe, B. Julsgaard, A. Walther, Y. Ying, and S. Kröll, Experimental quantum-state tomography of a solid-state qubit, Phys. Rev. A **77**, 022307 (2008).
[27] Z. N. Gürkan and E. Sjöqvist, Realization of a holonomic quantum computer in a chain of three-level systems, Phys. Lett. A **379**, 3050 (2015).
[28] D. Kult, J. Åberg, and E. Sjöqvist, Noncyclic geometric changes of quantum states, Phys. Rev. A **74**, 022106 (2006).
[29] $\mathcal{H}_{\Delta}(t)$ can be obtained from the original Hamiltonian $\mathcal{H}(t)$ in Eq. (1) by setting $\Upsilon_p = \Omega(t)\omega_p$ and $\Delta_0 = \Delta_1 \equiv -\Delta$ and adding a trivial zero-point energy term $\Delta\hat{1}$.
[30] I. Roos and K. Mølmer, Quantum computing with an inhomogeneously broadened ensemble of ions: Suppression of errors from detuning variations by specially adapted pulses and coherent population trapping, Phys. Rev. A **69**, 022321 (2004).
[31] J. Spiegelberg and E. Sjöqvist, Validity of the rotating-wave approximation in nonadiabatic holonomic quantum computation, Phys. Rev. A **88**, 054301 (2013).
[32] We demonstrate explicitly why $\pi/2$ pulses are essential for the two path segments to form a loop in the Grassmannian. To this end, we evaluate the time-evolution operators $\mathcal{U}_1(a_1,0)$ and $\mathcal{U}_2(a_2,0)$ for the two sets of initial vectors $|\psi_{1,k}(0)\rangle$ and $|\psi_{2,k}(0)\rangle$, respectively, in the $L=2$ setting. We obtain $\mathcal{U}_1(a_1,0) = |d\rangle\langle d| + \cos a_1(\hat{1} - |d\rangle\langle d|) - i\sin a_1(|b\rangle\langle e| + |e\rangle\langle b|)$ and $\mathcal{U}_2(a_2,0) = |d\rangle\langle d| + \cos a_2(\hat{1} - |d\rangle\langle d|) - i\sin a_2(e^{-i\eta}|b\rangle\langle e| + e^{i\eta}|e\rangle\langle b|)$. The combined pulse pairs correspond to a loop, provided $\mathcal{U}_2(a_2,0)\mathcal{U}_1(a_1,0)\mathbb{P}(0) = |d\rangle\langle d| + (\cos a_1\cos a_2 - e^{-i\eta}\sin a_1\sin a_2)|b\rangle\langle b|$ is unitary. This is the case if $1 = |\cos a_1\cos a_2 - e^{-i\eta}\sin a_1\sin a_2|^2 = \sin^2(\frac{\eta}{2})\cos^2(a_1 - a_2) + \cos^2(\frac{\eta}{2})\cos^2(a_1+a_2)$. Thus, a_1 and a_2 must be integer multiples of $\pi/2$ such that $a_1 - a_2$ and $a_1 + a_2$ are integer multiples of π.